# Nonlinear compression of picosecond chirped pulse from thin-disk amplifier system through a gas-filled hollow-core fiber*

Jun Lu(陆俊)[1,2,3], Zhi-Yuan Huang(黄志远)[2,4], Ding Wang(王丁)[2], Yi Xu(许毅)[2], Yan-Qi Liu(刘彦祺)[2], Xiao-Yang Guo(郭晓杨)[2], Wen-Kai Li(黎文开)[2], Fen-Xiang Wu(吴分翔)[2], Zheng-Zheng Liu(刘征征)[2], and Yu-Xin Leng(冷雨欣)[2,†]

[1] *School of Physics Science and Engineering, Tongji University, Shanghai* 200092, *China*
[2] *State Key Laboratory of High Field Laser Physics, Institute of Optics and Fine Mechanics, Chinese Academy of Sciences, Shanghai* 201800, *China*
[3] *University of Chinese Academy of Sciences, Beijing* 100049, *China*
[4] *Department of Physics, Shanghai University, Shanghai* 200444, *China*

(Received 30 May 2016; revised manuscript received 15 July 2016; published online 25 October 2016)

We theoretically study the nonlinear compression of a 20-mJ, 1030-nm picosecond chirped pulse from the thin-disk amplifier in a krypton gas-filled hollow-core fiber. The chirp from the thin-disk amplifier system has little influence on the initial pulse, however, it shows an effect on the nonlinear compression in hollow-core fiber. We use a large diameter hollow waveguide to restrict undesirable nonlinear effects such as ionization; on the other hand, we employ suitable gas pressure and fiber length to promise enough spectral broadening; with 600-μm, 6-bar (1 bar = $10^5$ Pa), 1.8-m hollow fiber, we obtain 31.5-fs pulse. Moreover, we calculate and discuss the optimal fiber lengths and gas pressures with different initial durations induced by different grating compression angles for reaching a given bandwidth. These results are meaningful for a compression scheme from picoseconds to femtoseconds.

**Keywords:** picosecond pulse, hollow-core fiber, thin-disk amplifier, spectrum broadening

**PACS:** 42.65.Re, 42.65.Jx, 42.81.Qb, 42.55.Xi **DOI:** 10.1088/1674-1056/25/12/124207

## 1. Introduction

The thin-disk laser has been used as an important laser technology for scientific research,[1–4] medical,[5] and industry application[6–9] since its invention by Giesen[10] *et al.* Over the past few years with the pump laser diodes power increasing while the price decreases drastically,[11] the thin-disk laser has been widely used in industries, for it combines the properties of excellent beam quality, high optical-optical efficiency, good thermal management, high average power, as well as high reliability, and moderate cost.[12] Thanks to the thin-disk technology, its unique aspect ratio of the laser crystal allows the heat to be removed from the disk efficiently. On the other hand, cooling from the rear side of the crystal makes the temperature distribution on the disk nearly a one-dimensional heat flow which allows the laser operated in a very good mode. Another typical character of a thin-disk is the ease of the power scaling. By expanding the diameter of the pump laser while keeping the pump intensity constant we can achieve the power scaling easily.[13] Apart from this, power scaling can also be maintained through using multiple crystals in a single cavity. By carefully designing the cavity, we can easily operate the laser in fundamental mode which will benefit the user a lot. However, for some fundamental scientific researches, such as the high-harmonic generation (HHG),[14] the generation of bright x-ray,[15] time-resolved attosecond spectroscopy,[16] and pump-probe analysis,[17] the ultra-short few-cycle pulse is desired. But in the case of a thin-disk laser, its typical pulse duration is limited to a few picoseconds.

To achieve a shorter pulse, the external spectral broadening is needed. So far, lots of spectral broadening techniques have been developed, such as filamentation,[18] planar waveguide,[19] bulk material,[20] and hollow-core fiber (HCF).[21,22] Among them, the compression through a noble gas-filled HCF is widely used as it can compress the millijoule picosecond pulse down to the femtosecond level while keeping a comparatively good beam quality. Nowadays, HCF is mainly used to compress a tens of femtoseconds' pulse to few-cycles' pulse.[23] However, with the development of a high average power laser system, more work needs doing in the field of pulse compression from picoseconds to femtoseconds.[24,25]

In this paper, we theoretically study the nonlinear compressions of 20-mJ, 1-kHz picosecond pulses with different chirp factors through a krypton gas-filled HCF. In Section 2 we describe the schematic layout of 20-mJ, 1-kHz thin-disk amplification system and the model of nonlinear compression by gas filled HCF. In Section 3, firstly, we show how to obtain the initial picosecond chirped pulse after the thin-disk amplifier system, then we investigate the influences of gas pressure,

*Project supported by the National Basic Research Program of China (Grant No. 2011CB808101), the Funds from the Chinese Academy of Sciences, and the National Natural Science Foundation of China (Grant Nos. 11127901, 10734080, 61221064, 60908008, and 61078037).

†Corresponding author. E-mail: lengyuxin@siom.ac.cn

© 2016 Chinese Physical Society and IOP Publishing Ltd 

inner diameter and fiber length on pulse width and spectral broadening for selecting the suitable parameters to compress the picosecond pulse. Moreover, we discuss the relation between initial durations induced by different compressor angles and fiber parameters including fiber length and gas pressure for reaching the same Fourier transform limited pulse width. We draw some conclusions in Section 4 finally.

## 2. Layout of kHz amplifier system and model of spectrum broadening

The 20-mJ, 1-kHz chirped pulse amplification (CPA) system includes a seeding laser operating at 1030 nm, an offner type stretcher, a pulse picker, a thin-disk standing-wave regenerator amplifier and a Treacy-type compressor as shown in Fig. 1. The seed laser comes from a commercial Ti:sapphire solid-state oscillator (Mira 900, coherent) which is characterized with a tens of nanometers' bandwidth, 110-fs pulse width and 80 megahertz repetition. The seed is then stretched by an Offner-type stretcher with a chirp factor of 210 ps/nm. Then the stretched pulse sequence is chosen to be 1 kHz by a pulse picker. After the stretcher, the seed has a 0.5-nJ energy and 10-nm spectral bandwidth. Afterwards the pulse is injected into a regenerator, which contains a faraday rotator to separate the incoming pulse from the outgoing pulse, and a Pockels cell with double 20-mm-thick BBO crystal and a clear aperture of 5.8 mm×5.8 mm to couple out an amplified pulse from the regenerator. An approximately 215-μm-thick Yb:YAG thin disk provided by Dausinger + giesen GmbH is used as a gain medium. The 7-at.% doped Yb:YAG disk has a diameter of 12 mm and a radius of −7 m. The disk is pumped with continuous wave (CW) fiber-coupled diodes with a 3.2-mm-diameter pumping spot at a wavelength of 940 nm with a near-flat-top profile. With a pump power of 300 W, a pulse with an energy of 20 mJ, a pulse width of 2 ps and repetition of 1 kHz is expected after being compressed with the grating pair.

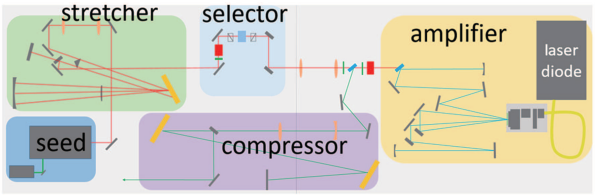



**Fig. 1.** (color online) Schematic layout of 20-mJ, 1-kHz thin-disk amplifier system.

In the thin-disk laser, the material dispersion is mainly introduced by BBO crystal and YAG crystal. The Sellmeier equation for BBO crystal[26,27] and YAG crystal are, respectively, as follows:

$$n^2_{\mathrm{BBO}}(\mathrm{o}) = 2.7359 + \frac{0.01878}{\lambda^2 - 0.01822} - 0.01471\lambda^2 + 0.0006081\lambda^4 - 0.00006740\lambda^6, \quad (1)$$

$$n^2_{\mathrm{YAG}} = 1 + \frac{2.28200\lambda^2}{\lambda^2 - 0.01185} + \frac{3.27644\lambda^2}{\lambda^2 - 282.734}, \quad (2)$$

where $n_{\mathrm{BBO}}(\mathrm{o})$ and $n_{\mathrm{YAG}}$ are refractive index in normal light in BBO crystal and YAG crystal, respectively; $\lambda$ is the center wavelength of the thin disk laser in micron. Dispersions introduced by stretcher and compressor[28] are calculated as follows:

$$\varphi^2(\omega_0) = \frac{2bG^2}{c\omega_0}, \quad (3)$$

$$\varphi^3(\omega_0) = -\frac{3}{\omega_0}\varphi^2(\omega_0)\cdot[1 + G\cdot\tan(\rho_0)], \quad (4)$$

$$\varphi^4(\omega_0) = -\frac{3}{\omega_0^2}\varphi^2(\omega_0)\cdot\{4 + 8G\cdot\tan(\rho_0) + G^2\cdot[1 + 5\tan^2(\rho_0)]\}, \quad (5)$$

where $\varphi^2(\omega_0)$, $\varphi^3(\omega_0)$, and $\varphi^4(\omega_0)$ are corresponding to Group dispersion delay (GDD), the third order dispersion (TOD), and the fourth order dispersion (FOD) respectively; $b$ is the slant distance between two gratings; G is the perpendicular distance between the gratings of the grating pair; $\omega_0$ is the center angular frequency; $\rho_0$ is the diffraction angle.

The spectral broadening is based on self-phase modulation (SPM) through a noble gas-filled HCF. The envelop $E(z,t,r)$ of the light is assumed to vary slowly with time, and evolves through the propagation direction z following the fundamental mode equation of propagation.[29,30]

$$\frac{\partial E}{\partial z} = \mathrm{i}\hat{L}E + \mathrm{i}\hat{T}\left(\frac{\omega_0}{c}n_2\gamma|E|^2E\right) - \left[\frac{\sigma}{2}\mathrm{d}E + \frac{\mathrm{i}q_{\mathrm{e}}^2}{2c\omega_0 m_{\mathrm{e}}\varepsilon_0}\hat{T}^{-1}(\mathrm{d}E)\right] - \frac{f}{2|E|^2}E, \quad (6)$$

where the waveguide mode attenuation is described by the linear operator $\hat{L} = \mathrm{i}\alpha^{(0)} - \alpha^{(1)}\partial/\partial_\tau + \sum_{m=2}^{\infty}(\mathrm{i}^m\partial^m/\partial_{\tau^m})[\beta^{(m)} + \mathrm{i}\alpha^{(m)}]/m!$, $\alpha^{(m)} = \mathrm{d}^m\alpha/\mathrm{d}\omega^m|_{\omega=\omega_0}$, and dispersion parameter $\beta^{(m)} = \mathrm{d}^m\beta/\mathrm{d}\omega^m|_{\omega=\omega_0}$ with center angular frequency $\omega_0$, with $\tau = t - z/v_{\mathrm{g}}$ referring to retarded time and group velocity being $v_{\mathrm{g}} = 1/\beta^{(1)}$. Constants such as $c$, $\sigma$, $q_{\mathrm{e}}$, $m_{\mathrm{e}}$, and $\varepsilon_0$ represent the light speed in a vacuum, impact ionization cross section, electron charge, mass, and vacuum permittivity, respectively. The operator $\hat{T} = 1 + (\mathrm{i}/\omega_0)(\partial/\partial_\tau)$ introduces the self-steeping effects, while $n_2$ refers to the nonlinear index of refraction. The coefficient $g = \int_0^a V^4\times r\mathrm{d}r/\int_0^a V^2\times r\mathrm{d}r$ with pulse transverse mode $V = \mathrm{J}_0(ur/a))$, where $r$, $a$ are the transverse coordinate and fiber inner radius, $\mathrm{J}_0(x)$ is the zero-order Bessel function of the first kind, and $u$ is the first zero point of $\mathrm{J}_0(x)$. Parameters $d = \int_0^a \rho V^2\cdot r\mathrm{d}r/\int_0^a V^2\cdot r\mathrm{d}r$ and $f = \int_0^a W(\rho_{nt} - \rho)U_p\cdot r\mathrm{d}r/\int_0^a V^2\cdot r\mathrm{d}r$, where $\rho$ is the density of electron, $W$ is the ionization rate, $\rho_{nt}$ is the neutral density of the gas, and $U_p$ is the ionization potential. The terms on the right-hand side (RHS) of Eq. (7) take account of losses, high order dispersion, self-focusing due to the Kerr effect and

self-steeping, defocusing due to plasma, and energy absorption due to ionization. Assuming that electrons born at rest, electron density evolves as

$$\frac{\partial \rho}{\partial t} = W(\rho_{nt} - \rho) + \frac{\sigma}{U_p}\rho |E|^2 . \quad (7)$$

Ionization rate $W$ is achieved through Perelomov, Popov and Terent'ev (PPT) theory.[31]

## 3. Numerical results and analysis

Firstly, we calculate GDD, TOD, FOD introduced by the thin-disk amplifier system. The material dispersion is mainly introduced by the standing wave regenerator with pulse oscillating nearly 100 round trips. BBO crystal in the cavity is 40 mm in length and the thin disk crystal is about 0.215-mm thick. For each round trip, the normal light travels through BBO crystal twice and V-pass four times for the thin-disk. The total lengths for BBO crystal and YAG crystal are 8000 mm and 172 mm, respectively. The dispersions per millimeter for YAG crystal and normal light for BBO crystal are shown in Table 1.

**Table 1.** Dispersions per mm for BBO and YAG crystal.

| Item | GDD/fs$^2$ | TOD/fs$^3$ | FOD/fs$^4$ |
|---|---|---|---|
| YAG | 66.6 | 67.3 | –42.9 |
| BBO(o) | 47.5 | 58.4 | –38.2 |

Then we calculate the dispersions introduced by the stretcher and compressor. The incident angle for the stretcher is 70.0°; in order to find the influence of mismatching between compressor and stretcher on the fiber compression, we calculate the dispersions introduced by the compressor with incident angle varying from 69.6° to 70.1°. Dispersions introduced in the laser system are shown in Table 2. The mismatching of incident angle between the stretcher and compressor is the main source of the chirped pulse.

Figure 2(b) shows the spectral intensity profile of the compressed pulse characterized with a center wavelength of 1030 nm and bandwidth of 1 nm, the spectrum is measured through USB 2000+(ocean optics). The blue solid curve in Fig. 2(a) represents the FTL pulse envelope, and the red dash curve corresponds to Gauss fitted pulse with the same pulse width of 1.558 ps.

**Table 2.** All dispersions of the system.

| Item | Incident angle | GDD/fs$^2$ | TOD/fs$^3$ | FOD/fs$^4$ |
|---|---|---|---|---|
| Oscillator | – | $6.17\times10^4$ | – | – |
| Material | – | $5.87\times10^5$ | $7.19\times10^5$ | $-4.70\times10^5$ |
| Stretcher | 70.0° | $1.09\times10^8$ | $-1.18\times10^9$ | $2.15\times10^{10}$ |
| Compressor | 69.6° | $-1.11\times10^8$ | $1.22\times10^9$ | $-2.25\times10^{10}$ |
| | 69.7° | $-1.11\times10^8$ | $1.21\times10^9$ | $-2.22\times10^{10}$ |
| | 69.8° | $-1.10\times10^8$ | $1.20\times10^9$ | $-2.20\times10^{10}$ |
| | 69.9° | $-1.10\times10^8$ | $1.19\times10^9$ | $-2.17\times10^{10}$ |
| | 70.0° | $-1.09\times10^8$ | $1.18\times10^9$ | $-2.15\times10^{10}$ |
| | 70.1° | $-1.09\times10^8$ | $1.17\times10^9$ | $-2.12\times10^{10}$ |

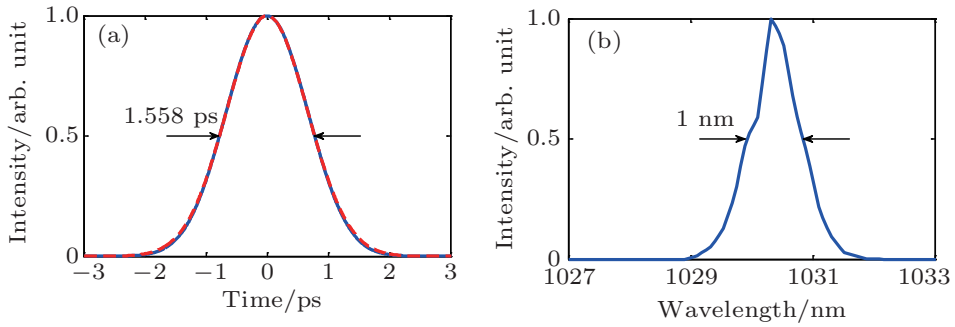



**Fig. 2.** (color online) (a) The FTL pulse and (b) spectral profile of the input pulse with an energy of 20 mJ at 1030 nm. Red dash curve represents Gauss fitted pulse, with a duration of 1.558 ps.

The blue solid curves in Figs. 3(a) and 3(b) show the temporal and spectral profile of the initial chirped pulse with an incident angle of 70.0° for stretcher and also compressor. Considering the dispersions introduced by the oscillator and material, the pulse is stretched to 1.939 ps. The corresponding spectral phase is shown in Fig. 3(b); as we can see, the pulse obtains a positive near-linear chirp.

Previously, Huang *et al.*[25] simulated the compression of a 10-mJ, 10-Hz, 5-ps pulse to 67 fs through krypton filled HCF. Based on his work, at first, we try to use a larger-inner-diameter krypton filled with HCF to compress the chirped picosecond pulse. Here we employ a root-mean-

square (RMS) value to describe the spectral broadening.[32] The spectral broadening factor due to HCF can be written as $\delta = \Delta\omega_{\rm rms}/\Delta\omega_0$, $\Delta\omega_{\rm rms}$, and $\Delta\omega_0$ represent the RMS spectral widths of output and input pulse, respectively, and they are defined, respectively, as follows:[33]

$$\begin{cases} (\Delta\omega)^2 = \langle(\omega-\omega_0)^2\rangle - \langle(\omega-\omega_0)\rangle^2, \\ \langle(\omega-\omega_0)^n\rangle = \dfrac{\int_{-\infty}^{\infty}(\omega-\omega_0)^n I(\omega)\,{\rm d}\omega}{\int_{-\infty}^{\infty} I(\omega)\,{\rm d}\omega}, \end{cases} \tag{8}$$

where $I(\omega)$ is the spectral intensity, and $\omega_0$ is calculated by

$$\omega_0 = \int_{-\infty}^{\infty} \omega I(\omega)\,{\rm d}\omega \Big/ \int_{-\infty}^{\infty} I(\omega)\,{\rm d}\omega.$$

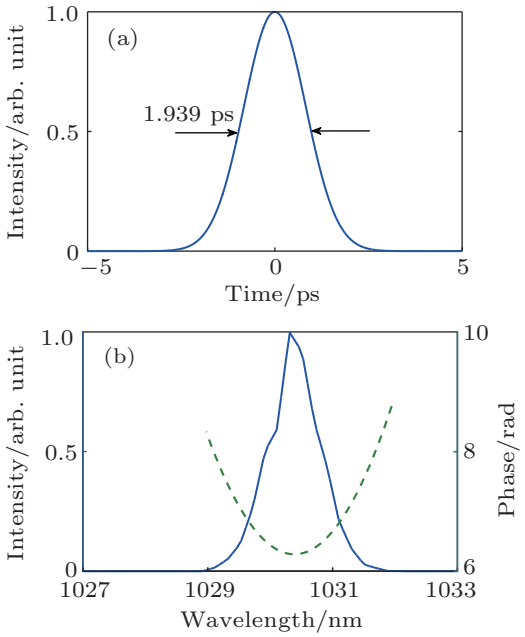



**Fig. 3.** (color online) (a) Temporal and (b) spectral profile of the input pulse with initial chirped duration of 1.939 ps at compressor angle of 70°, with the green dash curve corresponding to phase distribution.

Figure 4 shows the spectral broadening factor (blue circle curve) and FTL duration (green square curve) of the output pulse with gas pressure increasing from 0.3 bar (1 bar = $10^5$ Pa) to 3 bar. Broadening factor presents a linear relation with gas pressure, and the slope of FTL duration shows that the pulse can be compressed to 100 ps∼200 fs as well as a few tens of femtoseconds, but it makes more effort to achieve the shorter one. Figure 5 gives the temporal and spectral intensity profile of the output pulse. When paying attention to the red solid curve in Fig. 5(a), we can observe some oscillation appearing near the peak of the pulse, which is induced by the ionization effect.[34,35] With increasing gas pressure, the enhanced oscillation will restrict the compressed pulse quality. To suppress this effect, we present the relation between the temporal profile and fiber inner diameter as shown in Fig. 6. For 600-μm inner diameter fibers, even with 10-bar gas pressure in HCF, the output pulse still obtains an excellent temporal profile.

Figures 7(a) and 7(b) show the variations of FTL duration of output pulse with gas pressure (blue square curve) and fiber length (red circle curve), respectively. The fiber length and inner diameter are 1-m and 600 μm, respectively, and the pressure is 6-bar. In order to obtain shorter duration, we need to use the large gas pressure to promise enough spectral broadening.

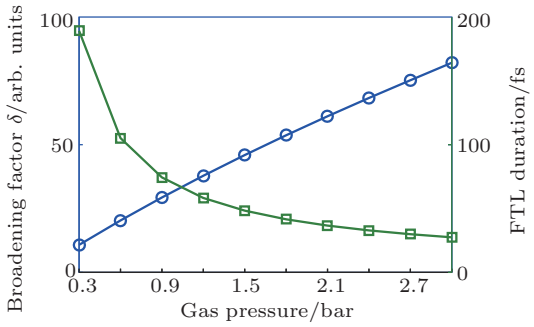



**Fig. 4.** (color online) Broadening factor (blue circle curve) and FTL duration (green square curve) of the output pulse for fiber inner diameter of 400 μm, and fiber length of 1 m.

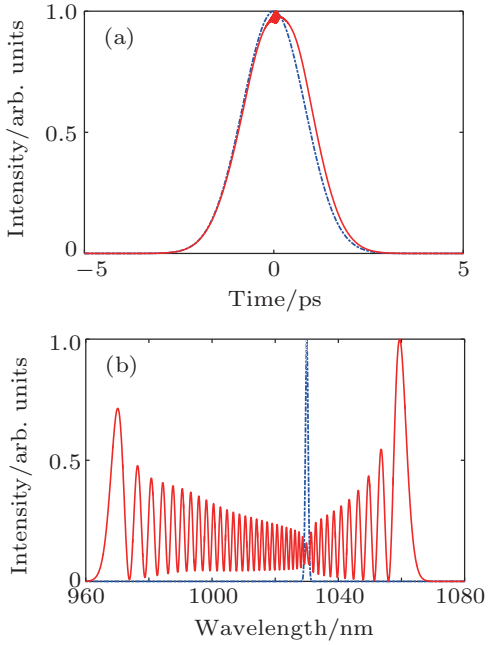



**Fig. 5.** (color online) (a) Temporal profiles for input (blue dash curve) and output (red solid curve) pulse, respectively. (b) Spectral intensity profiles of the input (blue dash curve) and output (red solid curve) pulse, respectively. The fiber inner diameter is 400 μm, fiber length is 1 m, and gas pressure is 3 bar.

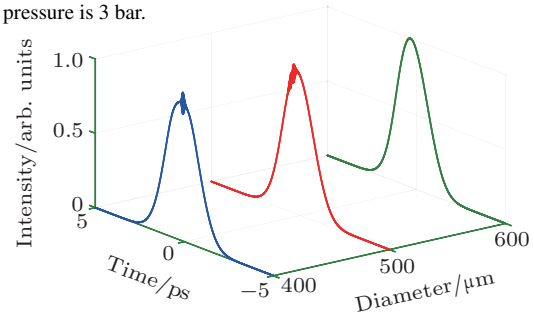



**Fig. 6.** (color online) Temporal profile evolutions with increasing of fiber inner diameter, gas pressures for fibers with diameters of 400 μm, 500 μm, and 600 μm, corresponding pressures are 4 bar, 5 bar, and 10 bar, respectively. The fiber length is 1 m.

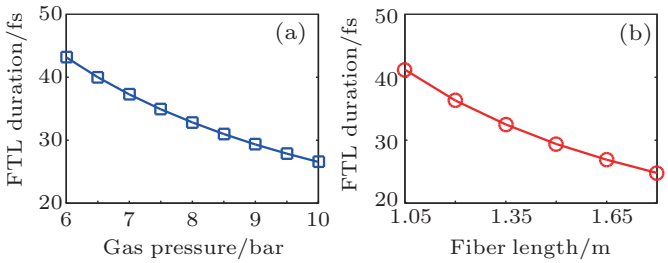



**Fig. 7.** (color online) (a) Variation of FTL duration of the output pulse with gas pressure for a fiber length of 1m and inner diameter of 600 μm, and (b) fiber length for gas pressure of 6 bar and inner diameter of 600 μm.

In addition, we can also increase the propagation length to reach the same bandwidth at a suitable gas pressure as shown in Fig. 7(b). Through simulation, we find that by using a 1.8-m fiber at a pressure of 6-bar, a pulse with a bandwidth of nearly 100 nm can be obtained, the corresponding FTL duration reaches 24.8 fs, as shown by the blue solid curve in Fig. 8(b) and by the black dash curve in Fig. 8(a), respectively.

In the next step we are going to perform the experiment. The experiment setup is shown in Fig. 9. Firstly, we use a lens with a focal length of 0.9 m to focus the 3-mm diameter pulse into about 380 μm, so that we can guarantee a maximum coupling efficiency[36] into the 600-μm-diameter fiber, then we use three pairs of chirp mirrors to compensate for the redundancy GDD. After passing on the chirp mirror pairs three times, the pulse receives a total GDD of $-6000$ fs$^2$, afterwards we expect to obtain a pulse with a duration of 31.5 fs.

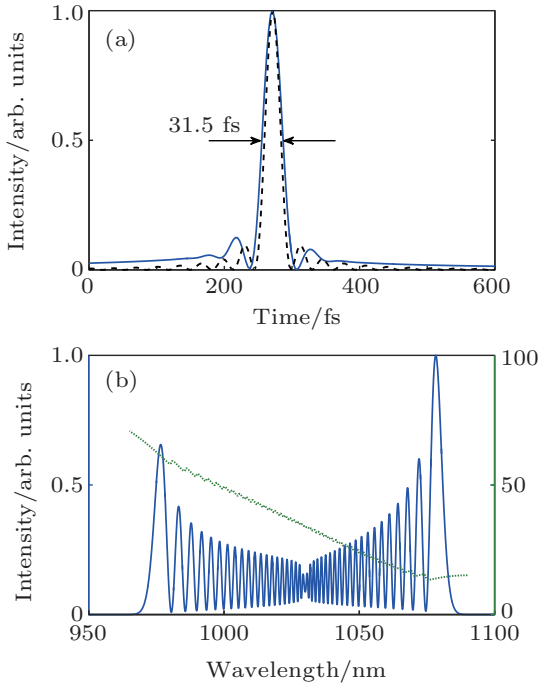



**Fig. 8.** (color online) (a) FTL pulse (black dash curve) and temporal profile (blue solid curve) of the compressed pulse. (b) The spectra intensity profile (blue solid curve) and phase distribution (green dotted curve) of the compressed pulse, with the fiber inner diameter being 600 μm, fiber length being 1.8 m, and gas pressure being 6 bar.

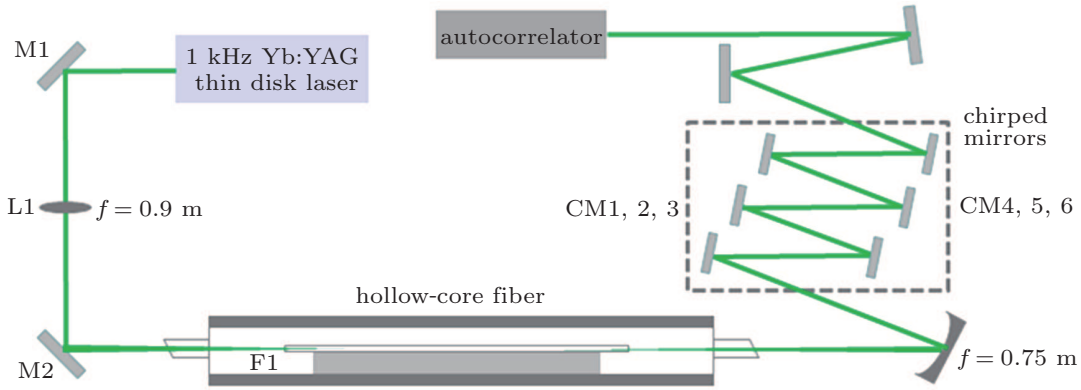



**Fig. 9.** (color online) Layout of fiber compressor, L1 is a lens with a focal length of 0.9 m, M1 and M2 are flat high reflective mirrors, and F1 is a fiber with a core diameter of 600 μm and length of 1.8 m.

On the other hand, a different incident angle of the grating compressor will introduce a different chirp in the pulse (see Table 2), resulting in various pulse durations. In the previous case, for compressor angle 70° (input duration 1.939 ps), to obtain the FTL duration 24.8 fs, the fiber parameters can be set to be (6 bar, 1.8 m), (6.5 bar, 1.67 m), or (7 bar, 1.55 m) as shown in Fig. 10.

Moreover, owing to a similar input duration, for angle 69.7° (1.942 ps), the corresponding parameters are (6 bar, 1.82 m), (6.5 bar, 1.68 m) or (7 bar, 1.56 m). But for angles 69.6° (2.434 ps) and 70.1° (2.431 ps), they have the larger durations, thus we need to increase gas pressure and fiber length for reaching the same FTL bandwidth, corresponding to the parameters (7 bar, 2.93 m), (7.5 bar, 2.51 m), (8 bar, 2.19 m), and (7 bar, 2.88 m), (7.5 bar, 2.46 m), (8 bar, 2.15 m), respectively. However, for angle 69.8° (1.581 ps) and 69.9° (1.620 ps), with the same input energy, the shorter pulse has the higher peak intensity that will enhance the ionization effect. Therefore, we should use the larger inner diameter such as 800 μm to suppress the oscillation. The used fiber parameters are (5 bar, 2.55 m), (5.5 bar, 2.33 m), (6 bar, 2.13 m), (5 bar, 2.67 m), (5.5 bar, 2.43 m), and (6 bar, 2.22 m), respectively.

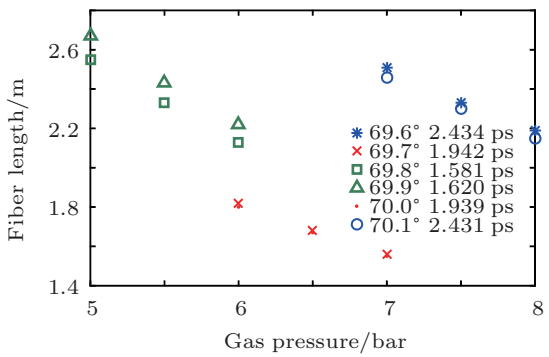



**Fig. 10.** (color online) Fiber lengths and gas pressures for compressor incident angle ranging from 69.6° to 70.1° and stretcher incident angle is 70.0° while compressing the pulse to FTL duration of 24.8 fs.

## 4. Conclusions

In this work, we theoretically study the nonlinear compression of picosecond chirped pulse from the thin-disk amplifier system based on krypton gas-filled HCF. We show how to choose the suitable HCF parameters to compress the initial picosecond pulse and also promise the compressed pulse quality. For a 20-mJ, 1.939-ps, 1030-nm chirped pulse, using 1.8-m fiber length and 6-bar gas pressure, after making $-6000$ fs$^2$ compensation, we obtain a compressed pulse duration of 31.5 fs. In addition, for the different initial pulse durations induced by various compressor angles, reaching a given FTL bandwidth (24.8 fs), we present and compare the corresponding fiber parameters including fiber length and gas pressure, which is useful for designing the HCF compression scheme.

## References


[1] Bartels A, Dekorsy T and Kurz H 1999 *Opt. Lett.* **24** 996
[2] Wu P, Sui C and Huang W 2014 *Photon. Res.* **2** 82
[3] Zapata L E, Reichert F, Hemmer M and Kaertner F X 2016 *High Intensity Lasers and High Field Phenomena,* March 20–22, 2016, California, USA, p. HM8B. 2
[4] Grant-Jacob J A, Beecher S J, Parsonage T L, Hua P, Mackenzie J I, Shepherd D P and Eason R W 2016 *Opt. Mater. Express* **6** 91
[5] Hoy C L, Durr N J, Chen P, Piyawattanametha W, Ra H, Solgaard O and Ben-Yakar A 2008 *Opt. Express* **16** 9996
[6] Kleinbauer J, Knappe R and Wallenstein R 2005 *Appl. Phys. B* **80** 315
[7] Malinauskas M, Žukauskas A, Bičkauskaitė G, Gadonas R and Juodkazis S 2010 *Opt. Express* **18** 10209
[8] Ni X, Anoop K, Bianco M, Amoruso S, Wang X, Li T, Hu M and Song Z 2013 *Chin. Opt. Lett.* **11** 093201
[9] Cao X, Jahazi M, Immarigeon J P and Wallace W 2006 *J. Mater. Proc. Technol.* **171** 188
[10] Giesen A, Hügel H, Voss A, Wittig K, Brauch U and Opower H 1994 *Appl. Phys. B* **58** 365
[11] Ladran A, Ault E, Beach R, Campbell J, Erlandson A, Felker A, Freitas B, Meier W, Telford S and Ebbers C 2007 *Lawrence Livermore National Laboratory Report UCRL-CONF,* May 04–09, 2008, CA, USA, p. 237006
[12] Giesen A and Speiser J 2007 *IEEE J. Sel. Top. Quantum Electron.* **13** 598
[13] Schad S, Gottwald T, Kuhn V, Ackermann M, Bauer D, Scharun M and Killi A 2016 *SPIE LASE,* March 17, 2016, CA, USA, p. 972615
[14] Lewenstein M, Balcou P, Ivanov M Y, L'huillier A and Corkum P B 1994 *Phys. Rev. A* **49** 2117
[15] Popmintchev T, Chen M C, Arpin P, Murnane M and Kapteyn H C 2010 *Nat. Photon.* **4** 822
[16] Drescher M, Hentschel M, Kienberger R, Uiberacker M, Yakovlev V, Scrinzi A, Westerwalbesloh T, Kleineberg U, Heinzmann U and Krausz F 2002 *Nature* **419** 803
[17] Xiao W, Lin S, Taguchi A K and Woodbury N W 1994 *Biochemistry* **33** 8313
[18] Houard A, Jukna V, Point G, André Y B, Klingebiel S, Schultze M, Michel K, Metzger T and Mysyrowicz A 2016 *Opt. Express* **24** 7437
[19] Chen J, Suda A, Takahashi E J, Nurhuda M and Midorikawa K 2008 *Opt. Lett.* **33** 2992
[20] Schmidt B E, Béjot P, Giguère M, Shiner A D, Trallero-Herrero C, Bisson É, Kasparian J, Wolf J P, Villeneuve D M and Kieffer J C 2010 *Appl. Phys. Lett.* **92** 121109
[21] Chen X, Jullien A, Malvache A, Canova L, Borot A, Trisorio A, Durfee C G and Lopez-Martens R 2009 *Opt. Lett.* **34** 1588
[22] Huang Z Y, Wang D, Dai Y, Li Y, Guo X Y, Li W K, Chen Y, Lu J, Liu Z and Zhao R 2016 *Opt. Express* **24** 9280
[23] Bohman S, Suda A, Kanai T, Yamaguchi S and Midorikawa K 2010 *Opt. Lett.* **35** 1887
[24] Krylov A, Chernysheva M A, Chernykh D S, Kryukov P G and Dianov E M 2013 *Laser Physics* **23** 075107
[25] Huang Z Y, Wang D, Leng Y X and Dai Y 2014 *Chin. Phys. B* **23** 124210
[26] Eimerl D, Davis L, Velsko S, Graham E and Zalkin A 1987 *J. Appl. Phys.* **62** 1968
[27] Zelmon D E, Small D L and Page R 1998 *Appl. Opt.* **37** 4933
[28] Wang C and Leng Y X 2013 *Chin. Phys. Lett.* **30** 044208
[29] Courtois C, Couairon A, Cros B, Marques J and Matthieussent G 2001 *Phys. Plasmas* **8** 3445
[30] Wang D, Leng Y X and Huang Z Y 2014 *J. Opt. Soc. Am. B* **31** 1248
[31] Perelomov A, Popov V and Terent'ev M 1966 *Sov. Phys. JETP* **23** 924
[32] Huang Z Y, Wang D, Leng Y X and Dai Y 2015 *Opt. Express* **23** 17711
[33] Pinault S C and Potasek M 1985 *J. Opt. Soc. Am. B* **2** 1318
[34] Fedotov A, Serebryannikov E and Zheltikov A 2007 *Phys. Rev. A* **76** 053811
[35] Saleh M F, Chang W, Hölzer P, Nazarkin A, Travers J C, Joly N Y, Russell P S J and Biancalana F 2011 *Phys. Rev. Lett.* **107** 203902
[36] Nubling R K and Harrington J A 1998 *Opt. Eng.* **37** 2454